

^{89}Y NMR study of the effect of Zn substitution on the spin dynamics of $\text{YBa}_2\text{Cu}_4\text{O}_8$

G. V. M. Williams, J. L. Tallon, and R. Meinhold

New Zealand Institute for Industrial Research and Development, P.O. Box 31310, Lower Hutt, New Zealand

A. Jánossy

Institute of Physics, Technical University of Budapest, H-1521 Budapest, Hungary

(Received 13 June 1994; revised manuscript received 10 April 1995)

Zn-substituted $\text{YBa}_2\text{Cu}_4\text{O}_8$ high-temperature superconductors have been probed by ^{89}Y nuclear magnetic resonance (NMR), susceptibility, and thermopower measurements. With ^{89}Y NMR we have been able to study the gap in the spin density of states using the real part of the spin susceptibility determined from the Knight shift as Zn is progressively substituted onto the plane copper site. Zn substitution results in a rapid decrease in T_c with a negligible decrease in the spin-gap energy and an inhomogeneous filling in of the gap in spin density of states.

The magnetic properties of high- T_c superconducting cuprates are unusual when compared to conventional s -wave BCS superconductors. In the normal state the electron spins are correlated leading to a spin susceptibility which is enhanced near the antiferromagnetic wave vector $Q=(\pi, \pi)$.¹ As the temperature is decreased a gap at low energy appears in the spin susceptibility of underdoped samples.^{2,3} Recent studies⁴⁻⁶ have shown that the pairing interaction in high-temperature superconductors could be spin mediated. It is therefore important to fully investigate the relationship between the spin behavior and superconductivity. Moreover, Loram *et al.*⁷ have shown from heat-capacity studies that the normal-state gap may be a gap in the total excitation spectrum and therefore responsible for the depression of T_c with progressive underdoping. Following these ideas we found that the gap in the spin density of states as probed by ^{89}Y NMR and the normal-state gap from the heat capacity are equal, have the same hole concentration dependence, and correlate with the depression in T_c in $\text{YBa}_2\text{Cu}_3\text{O}_{7-\delta}$, $\text{YBa}_2\text{Cu}_4\text{O}_8$, and $\text{Y}_2\text{Ba}_4\text{Cu}_7\text{O}_{15-\delta}$.⁸ In this paper we extend these studies to Zn-substituted $\text{YBa}_2\text{Cu}_4\text{O}_8$ and we report on susceptibility, thermopower, and ^{89}Y NMR measurements which show that Zn substitution leads to an inhomogeneous "filling in" of the gap in the spin density of states (DOS). The $\text{YBa}_2(\text{Cu}_{1-x}\text{Zn}_x)_4\text{O}_8$ superconductor is underdoped and the parent ($x=0$) compound has a T_c of 81 K which is rapidly depressed with increasing x . An advantage of the $\text{YBa}_2(\text{Cu}_{1-x}\text{Zn}_x)_4\text{O}_8$ system is that the oxygen stoichiometry is fixed while for the $\text{YBa}_2(\text{Cu}_{1-x}\text{Zn}_x)_3\text{O}_{7-\delta}$ superconductor the oxygen stoichiometry is variable which can lead to oxygen defects, distortions, and inhomogeneity.⁸ Furthermore, unlike the ^{63}Cu nucleus, the ^{89}Y nucleus does not have a quadrupole moment and hence the ^{89}Y NMR signal is not quadrupole broadened.

Single-phase samples were prepared by decomposing a stoichiometric mix of Y_2O_3 , $\text{Ba}(\text{NO}_3)_2$, CuO , and ZnO powders in air at 700 °C. The $\text{YBa}_2(\text{Cu}_{1-x}\text{Zn}_x)_4\text{O}_8$ samples were reacted for 6 h at 920 °C, 24 h at 930 °C, and a further 24 h at 930 °C in oxygen at a pressure of 6 MPa.⁹ All samples were reground after each sinter. ac-susceptibility and thermopower measurements (calibrated against a Pb stan-

dard) were performed on pellets at temperatures of 4 K to room temperature. The temperature dependence of the thermopower, which exhibits a marked enhancement with the opening of the spin gap, is reported elsewhere.¹⁰

The ^{89}Y NMR signal was measured between 80 K and room temperature using a Varian Unity 500 spectrometer with a 11.74 T superconducting magnet. The room-temperature measurements were made using magic angle spinning (MAS) with a Doty 5 mm high-speed MAS probe and spinning speeds of 10 kHz to reduce the ^{89}Y NMR line-width. Bloch decay spectra were acquired using a delay of 20 s between 90° pulses. Static temperature-dependent measurements were made by using a Doty 5 mm probe and ^{89}Y NMR spectra were acquired using the spin-echo technique with a 20 s delay at room temperature increasing to 150 s at 90 K. The NMR shifts were measured relative to a 1 M aqueous solution of YCl_3 which had a Larmor frequency of 24.49 MHz.

As shown in Fig. 1(a) substitution of Zn for Cu atoms in these samples results in a rapid decrease in T_c . From infrared measurements it has been deduced that Zn substitutes

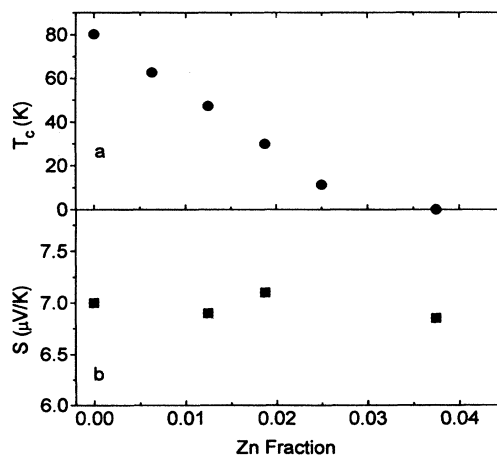


FIG. 1. (a) Superconducting diamagnetic transition temperature T_c for $\text{YBa}_2(\text{Cu}_{1-x}\text{Zn}_x)_4\text{O}_8$. (b) Room-temperature thermopower S for $\text{YBa}_2(\text{Cu}_{1-x}\text{Zn}_x)_4\text{O}_8$.

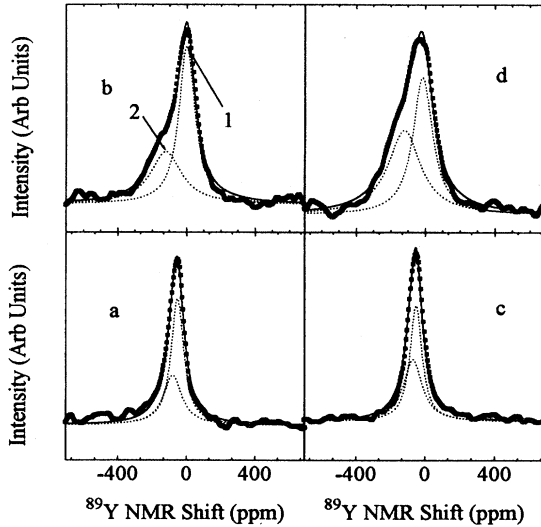


FIG. 2. ^{89}Y NMR shift for (a) $\text{YBa}_2(\text{Cu}_{3.9875}\text{Zn}_{0.0125})_4\text{O}_8$ at 293 K, (b) $\text{YBa}_2(\text{Cu}_{3.9875}\text{Zn}_{0.0125})_4\text{O}_8$ at 110 K, (c) $\text{YBa}_2(\text{Cu}_{3.9625}\text{Zn}_{0.0375})_4\text{O}_8$ at 293 K, and (d) $\text{YBa}_2(\text{Cu}_{3.9625}\text{Zn}_{0.0375})_4\text{O}_8$ at 110 K. The solid lines are fits to the model in the text. The dotted lines are the fitted ^{89}Y NMR signals from region near a Zn atom (satellite peak 2) and away from a Zn atom (main peak 1).

predominantly for plane Cu2 atom.¹¹ The room-temperature thermopower, which is a direct measure of the hole concentration,¹² is shown in Fig. 1(b) to be independent of Zn concentration implying that the decrease in T_c is not due to a decrease in hole concentration. If hole filling were responsible for the decrease in T_c , the thermopower would be expected to change from 7 to 80 $\mu\text{V}/\text{K}$ as T_c falls to zero.¹²

The ^{89}Y NMR spectra at 110 and 293 K for $\text{YBa}_2(\text{Cu}_{0.9875}\text{Zn}_{0.0125})_4\text{O}_8$ and $\text{YBa}_2(\text{Cu}_{0.9625}\text{Zn}_{0.0375})_4\text{O}_8$ are shown in Fig. 2. The asymmetry in the low-temperature spectra [(b) and (d)], which is not apparent in the room-temperature spectra [(a) and (c)], can be attributed to the Y atom probing two different environments.¹³ This asymmetry was not seen in the ^{89}Y NMR measurements on $\text{YBa}_2\text{Cu}_4\text{O}_8$. The ^{89}Y NMR spectra are fitted to two peaks labeled 1 and 2 in Fig. 2. The satellite resonance (peak 2) can be attributed to Zn inducing a local moment which then interacts with the nearest-neighbor Y atoms.¹³ Zn substitution is thought to lead to a local moment even though Zn is non-magnetic and the size of the induced moment can be as high as one Bohr magneton.¹⁴ In Fig. 3 we show the ^{89}Y NMR shifts for the satellite ^{89}Y resonance. Significantly, the shift is independent of Zn content and has a $1/T$ dependence. This is consistent with nearest-neighbor ^{89}Y atoms interacting with the moment induced by the Zn atom. using the Millis, Monien, and Pines¹⁵ model, the NMR shift of this resonance is modeled as,

$$K = (7D_{\text{Cu}}/g\mu_B)\chi_s + (D_{\text{Zn}}/g\mu_B)\chi_c + \sigma, \quad (1)$$

where D_{Cu} is the transferred hyperfine coupling constant from the spin on the Cu site to the ^{89}Y nuclei, D_{Zn} is the transferred hyperfine coupling constant from the local moment on the Zn site to the ^{89}Y nuclei, g is the electron g

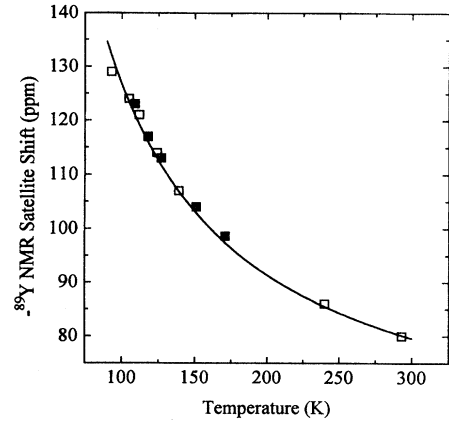


FIG. 3. ^{89}Y NMR shifts of the satellite resonance (peak 2 in Fig. 2) for the $\text{YBa}_2(\text{Cu}_{1-x}\text{Zn}_x)_4\text{O}_8$ samples with (\square) $x=0.0125$ and (\blacksquare) $x=0.0375$. The curve is a best fit curve to a Curie-like behavior of $a/T+b$.

factor, μ_B is the Bohr magneton, χ_s is the static susceptibility per CuO_2 unit due to the hyperfine interaction between Y and the electrons in the conduction band, χ_c is the static susceptibility of the induced moment per Zn atom, and σ is the chemical shift [152 ppm (Ref. 16)]. To obtain an estimate of the size of the local moment induced by Zn we take $D_{\text{Zn}}=D_{\text{Cu}}$ which implies that both the conduction-band wave functions and the Zn impurity wave functions at the Fermi level are similar. This assumption is consistent with the observation that both Cu and Zn have 3d outermost occupied levels. Furthermore as the thermopower is independent of Zn concentration then $N(E_f)$ and hence E_f are independent of Zn concentration which is consistent with the Zn-O orbital being within the Cu-O conduction band. The NMR shift data in Fig. 3 are modeled as $(7100/T+58)$ ppm as shown by the solid curve. Using the $\text{YBa}_2\text{Cu}_3\text{O}_{7-\delta}$ ^{89}Y hyperfine coupling constant, $D_{\text{Cu}}=-3.0$ kG,¹⁷ this corresponds to a Curie susceptibility of $\chi_c=4.4\times 10^{-25}/T$ emu/Zn atom. The size of the induced moment is estimated from the Curie molar susceptibility per Zn atom,

$$\chi_c = (\mu_B^2 P^2)/(3k_B T), \quad (2)$$

where P is the size of the induced moment per Zn atom. We find that the NMR shift of the satellite resonance (peak 2) corresponds to a moment of $\sim 0.9\mu_B$. A similar magnitude has been deduced for Zn-substituted $\text{YBa}_2\text{Cu}_3\text{O}_{6.64}$ ($P=0.6\mu_B$) which has a lower hole concentration¹³ and for Zn-substituted $\text{YBa}_2(\text{Cu}_{0.97}\text{Zn}_{0.03})_3\text{O}_7$ ($P\sim 1\mu_B$).¹⁴

The temperature dependence of the NMR shift of the main ^{89}Y resonance (peak 1 in Fig. 2) is plotted in Fig. 4 for $\text{YBa}_2(\text{Cu}_{1-x}\text{Zn}_x)_4\text{O}_8$ samples (open symbols) for four different Zn concentrations, $x=0$, $x=1.25\%$, $x=3.75\%$, and $x=5\%$. Increasing Zn content is shown by the arrow. We attribute this resonance to Y atoms that are not nearest neighbors to the Zn atoms. Also included in Fig. 4 are 245 GHz high-field ESR shift measurements made on $\text{Y}_{0.99}\text{Gd}_{0.01}\text{Ba}_2(\text{Cu}_{1-x}\text{Zn}_x)_4\text{O}_8$ samples¹⁸ (solid symbols). The exchange interaction with conduction electrons shifts the Gd^{3+} ($S=\frac{7}{2}$) ESR and the shift is proportional to the ^{89}Y Knight shift. At high magnetic fields crystal-field shifts are

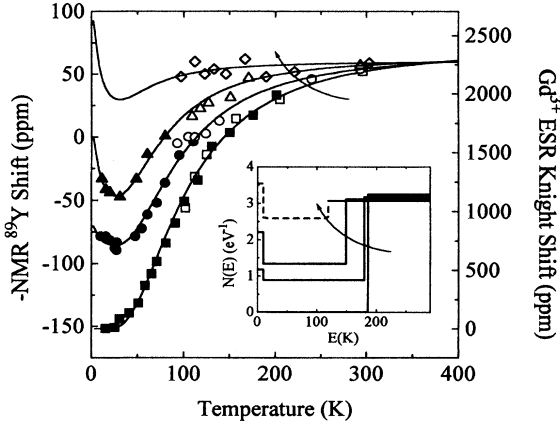


FIG. 4. ^{89}Y NMR shifts of the main resonance (peak 1 in Fig. 2) for $\text{YBa}_2(\text{Cu}_{1-x}\text{Zn}_x)_4\text{O}_8$ samples with (\square) $x=0$, (\circ) $x=0.0125$, (\triangle) $x=0.0375$, and (\diamond) $x=0.05$. Also included is Gd^{3+} ESR shifts of the central $-\frac{1}{2} \rightarrow +\frac{1}{2}$ transition (solid symbols) (Ref. 18). The solid curves are fits to Eq. (3) in the text. The K' , K_s , and E_0 values for the $x=0.05$ sample were estimated from the fits to the data for $x=0$, $x=0.0125$, and $x=0.0375$. The inset is the modeled density of states at low temperatures. The arrows indicate increasing Zn content.

negligible. Thus it is possible to use low-temperature ESR measurements to obtain low-temperature Knight shift data.^{19,20} To understand the NMR data we note that the NMR shift for a metal is $K_s + \sigma$ where K_s is the Knight shift. Only the Knight shift is temperature dependent and is proportional to the Pauli susceptibility $\mu_B^2 N(E_f)$ where $N(E_f)$ is the density of states at the Fermi level. For optimally doped superconductors K_s is constant as the temperature is reduced until the onset of superconductivity when K_s rapidly decreases to zero as $N(E_f)$ falls to zero. In the underdoped superconductor the Knight shift gradually falls to zero as the temperature

is reduced and this fall commences well above T_c , depending on the degree of underdoping. This behavior is associated with the opening of a gap in the spectrum of spin excitations observed by neutron-scattering measurements on $\text{YBa}_2\text{Cu}_3\text{O}_{7-\delta}$,^{2,3} phonon mode softening in $\text{Y}_{1-z}\text{Ca}_z\text{Ba}_2\text{Cu}_4\text{O}_8$ superconductors,²¹ heat-capacity and static-susceptibility measurements on $\text{YBa}_2\text{Cu}_3\text{O}_{7-\delta}$ (Refs. 7 and 22) and in the temperature-dependent enhancement of the thermopower of both $\text{YBa}_2\text{Cu}_2\text{O}_{7-\delta}$ and $\text{YBa}_2\text{Cu}_4\text{O}_8$.¹⁰

It can be seen in Fig. 4 that the zero-temperature Knight shift for the main resonance increases with Zn substitution. Similar behavior has been noted by Loram *et al.*²² in the temperature dependence of both the static susceptibility and S^{el}/T , where S^{el} is the electronic entropy, and this was attributed to filling in of the normal-state gap. Following their approach we model the NMR data by noting that the spin susceptibility $\chi_s(\mathbf{q}, \omega)$ can be expressed as

$$\chi_s = \mu_B^2 \int N(E) [-\partial f(E)/\partial E] dE, \quad (3)$$

in the long-wavelength and low-frequency limit where $f(E)$ is the Fermi function. We are able to satisfactorily fit the temperature dependence of $K(T)$ by modeling the DOS as a single step function at the gap energy E_g . To account for the experimentally observed gradual opening of the gap as temperature is reduced^{10,23} the depth of the step is described by a factor $[1 - \tanh(E_g/2kT)]$. This yields a Knight shift varying as $[1 - \tanh^2(E_g/2kT)]$ which is the phenomenological dependence proposed by Mehring²⁴ and used in our previous study.⁸ However the upturn in $K(T)$ at low temperatures for the Zn-substituted samples appears to be real and points to additional low-energy weight in the density of states as also noted by Loram²⁵ in modeling the static susceptibility of $\text{YBa}_2(\text{Cu}_{1-x}\text{Zn}_x)_3\text{O}_{7-\delta}$. We therefore have fitted the susceptibility using a DOS with two step functions as shown in the inset of Fig. 4, one at a low energy E_0 (~ 10 K) and one at the gap energy E_g , viz.,

$$N(E) = \begin{cases} N' \tanh(E_0/2kT) + (N - N_0)[1 - \tanh(E_g/2kT)] + N_0, & 0 < E < E_0 \\ (N - N_0)[1 - \tanh(E_g/2kT)] + N_0, & E_0 \leq E < E_g \\ N, & E \geq E_g \end{cases} \quad (4)$$

where the energies E are now relative to the Fermi level, N is the high-energy DOS, N_0 is the low-temperature DOS in the gap induced by Zn substitution, and N' is the low-energy DOS. Thus the resultant NMR shift is, by integration,

$$K = K_s \text{sech}^2(E_g/2kT) + K_0 + K' \tanh(E_0/2kT) \tanh(E_g/2kT) + \sigma, \quad (5)$$

where $K_s = (8D\mu_B/g)(N - N_0)$, $K_0 = (8D\mu_B/g)N_0$, and $K' = (8D\mu_B/g)N'$. It is also possible to show that Eq. (5) will still result if the step in $N(E)$ has some curvature about E_g with a finite width ΔE , provided that $\Delta E \ll T/\tanh(E_g/2kT)$. This is consistent with infrared measurements on $\text{YBa}_2\text{Cu}_4\text{O}_8$ where $N(E)$ is broadened about

E_g at high temperatures and narrowed about E_g at low temperatures.²³ The density of states obtained by fitting the main resonance NMR shifts in Fig. 4 to Eq. (5) are shown in the inset of Fig. 4 for low temperatures and the solid curves in the main figure are the fitted $K(T)$ curves which match the data very well. The DOS shown in the inset confirms a low-temperature picture of a fully gapped spin spectrum in the pure compound which is progressively filled in with Zn substitution.

The fitted spin-gap energies for the main resonance are presented in Fig. 5(a). These are approximately constant for Zn substitution levels up to $x=0.0375$, above which the spin gap rapidly falls to zero. This is consistent with the model recently proposed in which the spin gap is locally suppressed

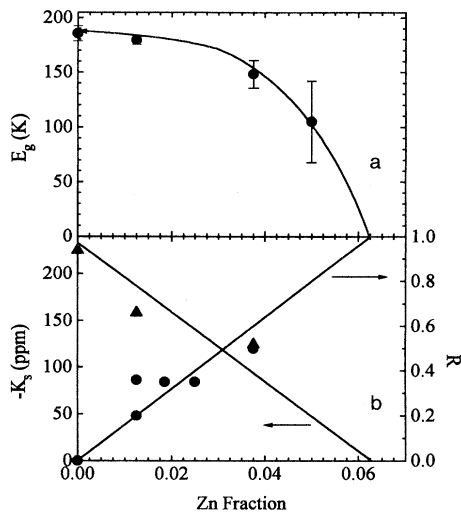


FIG. 5. (a) $\text{YBa}_2(\text{Cu}_{1-x}\text{Zn}_x)_4\text{O}_8$ fitted spin-gap temperatures E_g for peak 1 against Zn fraction. The solid line is a guide to the eye. (b) Fitted $\text{YBa}_2(\text{Cu}_{1-x}\text{Zn}_x)_4\text{O}_8$ K_s values from Eq. (5) (solid circles) and the fitted ratio of the ^{89}Y NMR integrated intensity of the satellite resonance (peak 1 in Fig. 2) divided by the total integrated intensity R (solid triangles) against Zn fraction. The solid lines are $K_s = K_s(x=0)(1-16x)$ and $R = 1 - 0.16x$, respectively.

about the Zn impurity but substantially unmodified in regions in the plane which are remote from the Zn atom.^{10,21} Moreover the radius of suppression must be very short, of the order of one lattice parameter a if E_g remains unchanged up to $x \approx 0.04$ where the mean spacing of Zn atoms is $3.5a$. Local suppression of the spin gap is also confirmed by the above analysis of the ^{89}Y NMR satellite resonance (peak 2 in Fig. 2) attributed to ^{89}Y adjacent to a Zn atom. The NMR shift data for the satellite resonance were fitted to $(7100/T + 58)$ ppm comprising only a Curie term and a constant Pauli paramagnetism term of 58 ppm. The absence

of any other temperature dependence implies the complete suppression of the spin gap near the Zn atom. A better estimate of the range of suppression of the spin gap about a Zn atom can be obtained from the data plotted in Fig. 5(b). Here we show the concentration dependence of the ratio R of the integrated ^{89}Y NMR intensity of the satellite peak to the total integrated ^{89}Y NMR intensity. Also shown is K_s obtained by fitting the main resonance data in Fig. 4 to Eq. (3). These data sets can be modeled as $R = 16x$ and $K_s = K_s(x=0)(1-16x)$ indicating that the gap in the spin spectrum is completely suppressed when $x = 0.0625$. For $x = 0.0625$ the Zn atoms are separated on each plane by, on average, $\sim 2.8a$, which occurs when adjacent Zn atoms share the same next-nearest neighbor at $1.4a$ which is comparable to the antiferromagnetic correlation length.²⁶ This implies that the spin gap is completely suppressed at nearest-neighbor sites to a Zn atom and is significantly suppressed at the next-nearest-neighbor sites.

In conclusion we have determined the spin susceptibility of $\text{YBa}_2(\text{Cu}_{1-x}\text{Zn}_x)_4\text{O}_8$ from temperature-dependent ^{89}Y -NMR Knight shifts in combination with Gd-ESR Knight shifts and the spin density of states is deconvoluted from the temperature dependence of the susceptibility. The Y resonance has a main peak associated with Y atoms well removed from Zn atoms and a satellite peak associated with Y atoms adjacent to a Zn atom. The shifts for the main resonance show the opening of the spin gap commencing above 200 K. The spin gap is “filled out” as the Zn concentration increases and is completely suppressed when, on average, Zn atoms share the same next-nearest neighbors at $x = 6.25\%$. In contrast, the satellite resonance shows that the spin gap is completely suppressed adjacent to a Zn atom at all concentrations and the range of suppression appears to be about $1.4a$.

We thank Dr. J. W. Loran and Dr. R. G. Buckley for helpful discussions on this work. This work has been funded by the New Zealand Foundation for Research, Science and Technology.

- ¹ P. B. Littlewood *et al.*, Phys. Rev. B **48**, 487 (1993).
- ² J. Rossat-Mignod *et al.*, Physica C **185-189**, 86 (1991).
- ³ J. M. Tranquada *et al.*, Phys. Rev. B **46**, 5561 (1992).
- ⁴ T. Moriya, Y. Takahashi, and K. Ueda, J. Phys. Soc. Jpn. **59**, 2905 (1990).
- ⁵ P. Monthoux and D. Pines, Phys. Rev. Lett. **69**, 961 (1992).
- ⁶ P. W. Anderson, Physica C **185-189**, 11 (1991).
- ⁷ J. W. Loram *et al.*, J. Supercond. **7**, 243 (1994).
- ⁸ J. L. Tallon *et al.*, Physica C **235-240**, 1821 (1994).
- ⁹ R. G. Buckley *et al.*, Physica C **174**, 383 (1991).
- ¹⁰ J. R. Cooper, J. L. Tallon, P. S. I. P. N. de Silva, and G. V. M. Williams (unpublished).
- ¹¹ R. G. Buckley (unpublished).
- ¹² S. D. Obertelli, J. R. Cooper, and J. L. Tallon, Phys. Rev. B **46**, 14 928 (1992).
- ¹³ A. V. Mahajan *et al.*, Phys. Rev. Lett. **72**, 3100 (1994).
- ¹⁴ R. E. Walstedt *et al.*, Phys. Rev. B **48**, 10 646 (1993).
- ¹⁵ A. J. Millis, H. Monien, and D. Pines, Phys. Rev. B **42**, 167 (1990).
- ¹⁶ M. Takigawa, W. L. Hults, and J. L. Smith, Phys. Rev. Lett. **71**, 2650 (1993).
- ¹⁷ H. Monien, D. Pines, and M. Takigawa, Phys. Rev. B **43**, 258 (1991).
- ¹⁸ A. Jánossy, A. Rockenbauer, L. Korecz, G. V. M. Williams, and J. L. Tallon (unpublished).
- ¹⁹ A. Jánossy, L.-C. Brunel, and J. R. Cooper (unpublished).
- ²⁰ A. Jánossy *et al.*, Phys. Rev. B **50**, 3442 (1994).
- ²¹ R. G. Buckley *et al.*, Physica C **235-240**, 1237 (1994).
- ²² J. W. Lorman *et al.*, *Advances in Superconductivity VII* (Springer-Verlag, Tokyo, in press).
- ²³ D. N. Basov *et al.*, Phys. Rev. B **50**, 351 (1994).
- ²⁴ M. Mehring, Appl. Magn. Reson. **3**, 383 (1992).
- ²⁵ J. L. Loram (private communication).
- ²⁶ J. Rossat-Mignod *et al.*, Phys. Scr. **45**, 74 (1992).